

Antiferromagnetic domains in $\text{YBa}_2\text{Cu}_3\text{O}_{6+x}$ probed by Gd^{3+} ESR

A. Jánossy, F. Simon, and T. Fehér

Technical University of Budapest, Institute of Physics, H-1521 Budapest, Post office box 91, Hungary

A. Rockenbauer and L. Korecz

Central Research Institute for Chemistry, H-1525 Budapest, Post office box 17, Hungary

C. Chen, A. J. S. Chowdhury, and J. W. Hodby

Clarendon Laboratory, Parks Road, Oxford, United Kingdom

(Received 17 March 1998)

The anisotropy of the static homogeneous magnetic spin susceptibility of the antiferromagnetic CuO_2 bilayers and the crystal-field parameters are measured in Gd-doped $\text{YBa}_2\text{Cu}_3\text{O}_{6+x}$ (small x) single crystals using Gd^{3+} ESR at 9, 75, 150, and 225 GHz. We show that the easy magnetization direction is along [100] and that there is a magnetostriction leading to an orthorhombic lattice distortion. We observe an antiferromagnetic domain structure corresponding to the two equivalent orthorhombic distortions of the tetragonal lattice which depends on magnetic fields of the order of 1 T. The domain structure is unchanged between 10 and 150 K and is independent of thermal and magnetic history. We discuss two models: (i) charged domain walls, (ii) magnetization pinned to a small number of defective oxygen-rich Cu(1) layers. [S0163-1829(99)01702-6]

I. INTRODUCTION

The nearly stoichiometric perovskite, $\text{YBa}_2\text{Cu}_3\text{O}_{6+x}$ with small values of x , is one of the best studied¹⁻⁴ antiferromagnetic (AF) parent compounds of superconductors. For $x=0$ it is an insulator with a half-filled band in which Coulomb interactions localize magnetic moments on the square lattice of Cu atoms of the CuO_2 bilayers. Superexchange antiferromagnetically couples neighboring Cu atoms *via* the O atoms with an exchange energy of $J=120$ meV.⁵ It is a model system for a quasi-two-dimensional antiferromagnet since magnetic coupling between neighboring bilayers is weak.

There is a large body of work on the magnetic structure. It is known that the AF magnetization lies in the (001) plane,⁴ therefore the crystal structure cannot be strictly tetragonal. The direction of the easy magnetization has not been determined and there has been no direct evidence for the coupling of the magnetization to the lattice.

Several authors have used the electron spin resonance (ESR) of Gd^{3+} to probe magnetic spin susceptibility and crystal fields of the CuO_2 bilayers of $\text{Gd:YBa}_2\text{Cu}_3\text{O}_{6+x}$. Gd^{3+} is an $S=7/2$ magnetic ion which substitutes for nonmagnetic Y^{3+} in-between the CuO_2 planes. It interacts only weakly with the antiferromagnetic layers and may be regarded as a nonperturbative probe. The Gd^{3+} fine structure was observed in $\text{Gd:YBa}_2\text{Cu}_3\text{O}_{6+x}$ by Causa *et al.*⁶ and single crystals were studied by Shaltiel *et al.*⁷ The tetragonal crystal-field parameters were determined with precision on oriented powders.^{8,9} The magnetic-spin susceptibility of $\text{Gd:YBa}_2\text{Cu}_3\text{O}_{6+x}$ oriented powders with various values of x determined from the shift of the Gd^{3+} ESR at high magnetic fields¹⁰ agrees well with ⁸⁹Y NMR shift measurements.¹¹

In this paper we present Gd^{3+} ESR data in a broad range of magnetic fields on high quality $\text{Gd:YBa}_2\text{Cu}_3\text{O}_{6+x}$ antiferromagnetic single crystals with small values of x . We measure the homogeneous static spin susceptibility along the

principal axes of the antiferromagnetic bilayers. We find that magnetostriction distorts the tetragonal symmetry of the crystal. There are no Cu(1)-O chains in the bulk of our samples and the distortion is not related to the structural orthorhombic distortion which occurs at higher oxygen concentrations. We observe a magnetic-field-dependent antiferromagnetic domain structure. At zero field, sublattice magnetization (M_s) and distortion are along [100] and the crystal consists of two types of domains with the [100] direction rotated by $\pi/2$. Applied magnetic fields of the order of 1 T strongly modify the domain structure. The main effect of the field is to rotate M_s from parallel to perpendicular to the field. The domain structure is independent of magnetic or thermal history and does not change in the temperature range of 10 to 150 K.

We discuss mechanisms which could lead to a hysteresis-free magnetic-field-dependent domain structure. One possibility is that domain walls are pinned to sheets of mobile holes localized in the bilayers and created by a small, uncontrolled concentration of oxygen in the Cu(1) planes. An entirely different possibility is that magnetic domains are determined by a small number of defective (**a,b**) planes and extend along the **c** direction.

II. SAMPLES AND EXPERIMENTAL DETAILS

We have studied the Gd^{3+} ESR of three single crystals of $\text{Gd}_{0.01}\text{Y}_{0.99}\text{Ba}_2\text{Cu}_3\text{O}_{6+x}$. Most features of the ESR spectra were the same for the three crystals and the same susceptibilities, crystal-field parameters and orthorhombic distortion were found. Two crystals were well-defined platelets with about 1 mm×1 mm surface and 0.1 mm thickness along **c** and these showed the same Gd^{3+} ESR spectra under identical conditions, i.e., for the same magnetic fields and temperatures.

The two principal (**a,b**) plane axes were interchangeable

in these crystals, i.e., the same spectra were recorded after a rotation of the magnetic field by 90 degrees in the (\mathbf{a}, \mathbf{b}) plane. [We denote by ‘‘principal axes in the (\mathbf{a}, \mathbf{b}) plane’’ the two directions fixed to the crystal which above the Néel temperature correspond to equivalent $[100]$ and $[010]$ directions. \mathbf{a}_t and $[110]_t$ denote the $[100]$ and $[110]$ directions of the tetragonal lattice, respectively. In the antiferromagnetic state there is a distribution of distortions and at zero magnetic field, a direction \mathbf{a}_t points along one of the inequivalent $[100]$ and $[010]$ directions depending on the local domain orientation. The principal axes of the distortion may be different from that of M_s for magnetic fields tilted from a principal axis into an arbitrary direction.] All data presented in this paper correspond to these two crystals. The third crystal was smaller and was less regular and the domain structure was not the same for magnetic fields along the two principal axes of the crystal in the (\mathbf{a}, \mathbf{b}) plane.

The nominal 1% Gd concentration agrees with the ESR linewidth which arises from Gd-Gd dipole interactions.⁸ The oxygen concentration x is not known and is probably a few % and is certainly not more than 15%. The as-grown single crystals were reduced at 800 °C in a dynamic vacuum for 72 h which normally reduces the oxygen content of the Cu(1) plane to a few %. The Gd^{3+} ESR spectrum, itself a sensitive indicator of oxygen doping, was consistent with a low concentration of oxygen. For $x > 0.15$ the variation of crystal fields of Gd^{3+} sites with different numbers of Cu(1)-O chain neighbors splits each component of the Gd^{3+} fine structure into well-defined lines.¹² No trace of oxygen chains has been detected in the ESR spectra of the present crystals.

The ESR spectra were recorded at the frequencies of 9, 75, 150, and 225 GHz with corresponding central transition Gd^{3+} resonance fields of about 0.3, 2.7, 5.4, and 8.1 T. All spectrometer functions and data collecting are computer controlled. At 9 GHz a conventional JEOL spectrometer was used and the sample was placed in a cavity and the derivative of absorption was detected. The high-frequency spectrometer has a quartz stabilized Gunn diode source at 75 GHz which is followed by a frequency doubler or a tripler for higher frequencies. At high frequencies the sample is placed onto a copper foil with a small amount of grease and is in helium exchange gas. In this setup a mixture of an absorption and a dispersion line is detected. We mixed a phase adjusted biasing wave into the mm wave reflected from the sample to get approximately an absorption line. Resonance positions of each component of the spectra were determined from a fit of a mixture of Lorentzian absorption and dispersion lines to the experimental spectra. In the fit the position, width and amplitude are free parameters for each line while the ratio of absorption to dispersion is a single fitting parameter for a full spectrum.

III. HAMILTONIAN FOR EXCHANGE INTERACTIONS AND CRYSTAL FIELDS AT THE Gd^{3+} SITES

The Zeeman energy is described by the usual effective spin Hamiltonian:

$$H_Z = \mu_B \mathbf{S} \cdot \text{Gd}^{\mathbf{g}} \cdot \mathbf{H}, \quad (1)$$

where \mathbf{S} is the effective $S=7/2$ spin for Gd^{3+} , $\text{Gd}^{\mathbf{g}}$ is the g tensor, and \mathbf{H} the applied external field. For magnetic fields

along the (θ, φ) polar angle directions with θ and φ measured from the \mathbf{c} and \mathbf{a} axes, respectively:

$$g(\theta, \varphi) = (g_a^2 \sin^2 \theta \cos^2 \varphi + g_b^2 \sin^2 \theta \sin^2 \varphi + g_c^2 \cos^2 \theta)^{1/2}. \quad (2)$$

For 1% concentration, Gd-Gd interactions are negligible for most of the Gd^{3+} ions.¹³ The exchange interaction of Gd^{3+} paramagnetic moments with the antiferromagnetic (AF) lattice shifts the resonance field. The shift is proportional to the homogeneous ($q=0$) susceptibility tensor of the bilayers χ :

$$H_{\text{ex}} = \text{Gd}^{\mathbf{g}} \mu_B \text{Gd}^{\mathbf{A}} \mathbf{S} \cdot \chi \cdot \mathbf{H}, \quad (3)$$

where $\text{Gd}^{\mathbf{A}}$ is a coupling constant proportional to the exchange interaction energy between Gd^{3+} and the AF bilayers. For simplicity in Eq. (3) we neglected the anisotropy of $\text{Gd}^{\mathbf{g}}$ and $\text{Gd}^{\mathbf{A}}$ although these may influence the spectrum measurably. We are not concerned in this paper by spin-lifetime effects which broaden the lines at high temperatures. At zero external magnetic field both exchange and dipolar fields of the antiferromagnetic lattice cancel to zero at the Gd site of the orthorhombic lattice.

Only an ‘‘effective’’ g tensor can be deduced from Eq. (3) since ESR shifts due to the spin susceptibility and the g anisotropy are not separable. Most of the shift from the free-electron value is isotropic, in a cubic environment Gd^{3+} ions have a characteristic g factor of 1.99 which is attributed¹⁴ to a 1% configurational mixing of the $P_{7/2}$ state to $S_{7/2}$. We estimate that the g anisotropy of our system produced by the spin-orbit coupling is negligible in the (\mathbf{a}, \mathbf{b}) plane, less than 0.0001, since as we show the orthorhombic distortion is very small, $b_2^2/b_2^0 = 0.038$. We assign the observed ‘‘effective’’ g anisotropy in the (\mathbf{a}, \mathbf{b}) plane entirely to the anisotropy of the antiferromagnetic susceptibility which is expected to be large. In the (\mathbf{a}, \mathbf{c}) plane the anisotropies described by Eqs. (2) and (3) cannot be separated using physical arguments.

Shifts are defined as $K = -(H_{\text{res}} - H_0)/H_0$ where H_{res} is the resonance field of the crystal and $H_0 = \omega/\gamma$ is a reference field with $\gamma = 2\pi g_0 \mu_B/h$. We used BDPA (*a,g*-bis(diphenyl)-*b*-phenylallyl) as a reference material. We assumed $\text{BDPA}^g = 2.00359$ and quote relative shifts with respect to $g_0 = 1.9901$ to be consistent with former work¹⁰ on $\text{Gd:YBa}_2\text{Cu}_3\text{O}_{6+x}$. We have tested that the resonance field of BDPA is temperature independent by measuring it together with dilute MnO/MgO (with a linewidth of 0.1 mT). The value of g_0 has an uncertainty of 0.001 as it depends on the precision of BDPA^g .

For tetragonal symmetry the crystal-field Hamiltonian is

$$H_{\text{tetra}} = 1/3 b_2^0 O_2^0 + 1/60 b_4^0 O_4^0 + 1/60 b_4^4 O_4^4 + 1/1260 b_6^0 O_6^0 + 1/1260 b_6^4 O_6^4. \quad (4)$$

Here $b_2^0, b_4^0, b_4^4, b_6^0, b_6^4$ are empirical crystal-field parameters. The $O_2^0, O_4^0, O_4^4, O_6^0, O_6^4$ spin operator equivalents are tabulated, e.g., in Refs. 14, 15. Twofold symmetric terms added to H_{tetra} take into account the orthorhombic distortion along a principal axis:

$$H_{\text{ortho}} = 1/3 b_2^0 O_2^0 + 1/60 b_4^0 O_4^0 + 1/1260 b_6^0 O_6^0 + 1/1260 b_6^6 O_6^6. \quad (5)$$

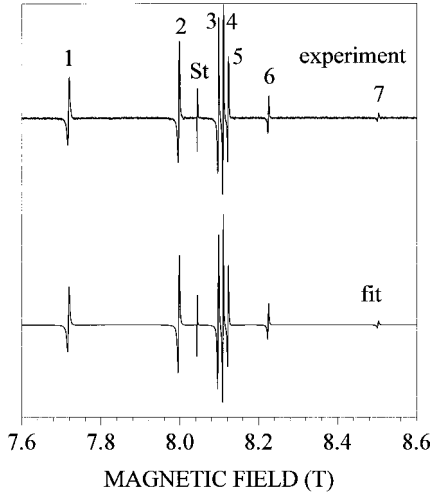


FIG. 1. Gd^{3+} ESR spectrum at 225 GHz and 25 K of $\text{Gd:YBa}_2\text{Cu}_3\text{O}_{6+x}$ for a magnetic field oriented along \mathbf{c} . Lines 1–7 are the fine-structure lines, St denotes the BDPA standard.

All observed ESR spectra were well described by taking into account only the $(1/3)b_2^2O_2^2$ term in Eq. (5) and we neglected higher-order distortions. $(1/3)b_2^2O_2^2$ in Eq. (5) is replaced by

$$H_{\text{ortho}} = 1/3 b_2^2 [\cos(2\alpha) \frac{1}{2}(S_+^2 + S_-^2) - i \sin(2\alpha) \frac{1}{2}(S_+^2 - S_-^2)], \quad (6)$$

when the principal axis of the orthorhombic distortion is inclined by an angle α from the $[100]$ direction of the undistorted tetragonal crystal. For an arbitrary orientation of the magnetic field, (θ, φ) , the direction of the distortion, α does not necessarily coincide with the direction of M_s .

IV. EXPERIMENTAL RESULTS

A. Magnetic field normal to the CuO_2 planes, $H \parallel \mathbf{c}$

The simplest spectra are obtained with the magnetic field oriented along \mathbf{c} (Fig. 1), i.e., with polar angle $\theta=0$. At 75 GHz and higher frequencies the crystal field is small compared to the Zeeman splitting and seven allowed fine-structure lines of the $S=7/2$ Gd^{3+} ions are observed. At low temperatures and high magnetic fields the higher energy Zeeman levels have strongly reduced populations and the inten-

sities of the corresponding transitions are small. The linewidth of all seven transitions is about 2 mT at 25 K showing that the quality of the crystals is very good. Strains or defects would broaden the lines through crystal-field effects, especially at the ends of the spectrum. A disorder in the antiferromagnetic structure would reduce the symmetry at the Gd sites and would broaden all lines by an equal amount.

Table I lists the parameters obtained from a large number of spectra with various field orientations and magnitudes. The tetragonal crystal-field parameters determined in this study agree well with the parameters measured⁹ on oriented powders at 9 and 35 GHz. For $H \parallel \mathbf{c}$ an orthorhombic distortion in the (\mathbf{a}, \mathbf{b}) plane affects the ESR spectrum only in high orders of b_2^2/H and a crystal-field Hamiltonian with tetragonal symmetry H_{tetra} describes all fine structure line positions at all frequencies. The crystal-field parameters are only slightly dependent on temperature.

B. Dependence on magnetic field in the $(\mathbf{a}_t, \mathbf{c})$ plane

For magnetic fields tilted from the normal of the (\mathbf{a}, \mathbf{b}) plane the spectra are split by an inhomogeneity of the magnetic susceptibility and crystal fields. The splitting of the fine structure in the $(\mathbf{a}_t, \mathbf{c})$ plane ($\varphi=0$ and arbitrary θ) has a simple interpretation. The interpretation of spectra at arbitrary angles, φ , discussed in Secs. IV C and IV D is more difficult.

The variation of the ESR spectrum measured at various frequencies with the magnetic field along \mathbf{a}_t ($\theta=\pi/2$) is shown in Fig. 2. Two series of fine-structure lines are clearly distinguished. One series is a set of seven sharp lines and has an increasing intensity with increasing field. The lines of the other series are broader and decrease in intensity with increasing field. For $\pi/2 > \theta > 0$ one also observes a narrower and broader series but with relative intensities depending on the component of the magnetic field along \mathbf{a}_t only (Fig. 3). For low magnetic fields the intensity ratio tends to 1 while for high magnetic fields only one set of narrow lines is observed. The relative intensity of the broader component at 5.4 T is about 0.01 and at 8.1 T the broader component was not observed anymore.

We assign the two series of fine-structure lines to antiferromagnetic domains. M_s lies closely along the $[100]$ easy direction in domains which differ in their orientation with respect to the applied magnetic field. M_s has for both types

TABLE I. Crystal-field parameters of $\text{Gd:YBa}_2\text{Cu}_3\text{O}_{6+x}$.

	b_2^0 (MHz)	b_2^2 (MHz)	b_4^0 (MHz)	b_4^4 (MHz)	b_6^0 (MHz)	b_6^4 (MHz)
25 K	-1265 ± 7	48 ± 9	-192 ± 3	817 ± 90	0.1 ± 0.6	-10 ± 6
75, 150, 225 GHz						
77 K	-1276 ± 1	48 ± 3	-190.7 ± 0.5	833 ± 5	1 ± 0.5	-10 ± 5
9, 75, 150, 225 GHz						
100 K	-1290 ± 6	43 ± 31	-191 ± 2	815 ± 7	0.3 ± 0.7	-9 ± 6
75, 225 GHz						
150 K	-1322 ± 9	40 ± 10	-191 ± 4	810 ± 13	1.2 ± 0.7	-16 ± 7
75, 150, 225 GHz						
77 K ^a	-1270	NA	-185.5	790	1.5	210
9.07 GHz						

^aReference 9; oriented powder of $\text{Gd}_{0.001}\text{Y}_{0.999}\text{Ba}_2\text{Cu}_3\text{O}_{6.06}$.

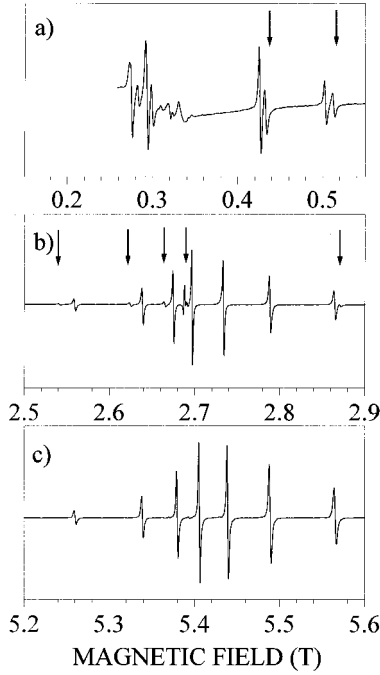


FIG. 2. Gd:YBa₂Cu₃O_{6+x} ESR spectra at 25 K for magnetic field along \mathbf{a}_1 , a principle axis in the (a,b) plane. (a) 9 GHz, (b) 75 GHz, (c) 150 GHz. Arrows indicate lines from antiferromagnetic domains with applied field along the easy magnetization direction, [100]. These are broader and also smaller in intensity than the unmarked lines from domains with magnetic field along [010]. At 9 GHz the staggered magnetization of domains is parallel or perpendicular to the field with comparable probability. At 150 GHz nearly all of the staggered magnetization is perpendicular to the applied field. At 9 GHz forbidden transitions complicate the spectrum below 0.35 T.

of domains an angular distribution around the [100] direction and this broadens the ESR lines. The series of sharper lines corresponds to domains for which the magnetic field is perpendicular to M_s . The broader lines of the second series correspond to domains for which the component of the magnetic field along \mathbf{a}_1 is approximately parallel to M_s .

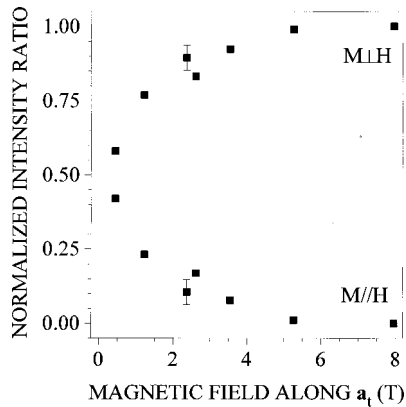


FIG. 3. Lower squares: normalized intensity ratio, $I_{\parallel}/(I_{\perp}+I_{\parallel})$, higher squares: $I_{\perp}/(I_{\perp}+I_{\parallel})$ of the fine-structure lines corresponding, respectively, to domains with staggered magnetization parallel and perpendicular to the component of the field in the (a,b) plane. Lower and higher squares are not independent experimental data but illustrate that perpendicular domains grow at the expense of parallel ones.

The measured magnetic susceptibilities and crystal-field parameters fully support this assignment. A single set of crystal-field parameters, including the orthorhombic distortion (Table I), and an anisotropic magnetic susceptibility (Table II) describe the resonance field values of both series in the (a,c) plane ($\varphi=0$) for various polar angles, θ , and resonance frequencies. The orthorhombic distortion b_2^2 is the same for the two types of domains but since the magnetic field has a different orientation, the magnetic susceptibilities are different. To verify this, the g factor and the magnitude of the distortion b_2^2 were determined for a large number of spectra recorded at various field orientations and frequencies. We assumed that although the distribution broadens the lines, the peak positions (i.e., the zero crossing of the derivative line) correspond to parallel or perpendicular domains. The exact orientation of the crystal with respect to the magnetic field was determined from the ESR spectra. The accuracy of the determination of the orientation was further checked by the Gd-Gd first- and second-neighbor dipolar spectra at low temperatures.¹³ Results for the two crystals are the same.

C. Low magnetic fields in the (a,b) plane, $H \perp c$

Low magnetic fields perturb the domain structure relatively little. A comparison of spectra at 9 GHz with magnetic field along \mathbf{a}_1 ($\varphi=0$ and $\pi/2$) and along [110], ($\varphi=\pi/4$ and $-\pi/4$) shows unambiguously that the distortion is along [100] and not along, say, [110] [Figs. 2(a) and Fig. 4]. The two series of lines in Fig. 2(a) correspond to domains with magnetic field along the [100] and [010] directions, respectively. The orthorhombic distortion along [100] splits the resonance fields of the two types of domains. Only one series of narrow lines is observed for a low magnetic field along the diagonal and this is the best proof for an easy magnetization direction along [100]. It shows that in spite of the distortion the [110] and [110] directions are equivalent.

The angular dependence of three fine-structure lines at 9 GHz is shown in Fig. 5. (The other lines are at lower fields where the spectra are complicated⁹). The solid curves are calculated using the tetragonal crystal-field parameters determined at higher frequencies (Table I) and a single orthorhombic parameter, $b_2^2=48$ MHz, to describe the distortion along [100]. For the calculation we assumed that M_s is not rotated with the magnetic field, however, we implicitly assumed that domain walls are displaced since the relative intensity of the two series changes. We neglected the distribution in the orientation of the distortion which, however, was observed in the spectra. Domains with the magnetic field along [010] have narrower lines (peak to peak linewidth, $\Delta H_{pp}=2.3$ mT), thus a narrower distribution than domains with fields along [100] ($\Delta H_{pp}=2.6$ mT). For intermediate directions the resonance field is more sensitive to variations of the distortion and lines are broader.

D. Magnetic fields in other directions

We have attempted to analyze some spectra for high magnetic fields with $0 < \varphi < \pi/2$ but have not performed a systematic study for arbitrary magnetic-field directions. In general two fine-structure series are distinguished. One series is

TABLE II. g factors, relative shifts of $\text{Gd:YBa}_2\text{Cu}_3\text{O}_{6+x}$.

	g_a	aK (ppm)	g_b	bK (ppm)	g_c	cK (ppm)
25 K	1.9924 ± 0.0002	1200 ± 100	1.988 21 $\pm 0.000 05$	-950 ± 25	1.98712 $\pm 0.000 05$	-1500 ± 25
100 K	1.9921 ± 0.0002	1000 ± 100	1.988 28 $\pm 0.000 06$	-910 ± 30	1.987 10 $\pm 0.000 07$	-1510 ± 35
150 K	1.9920 ± 0.0002	1000 ± 100	1.988 27 $\pm 0.000 06$	-920 ± 30	1.986 95 $\pm 0.000 06$	-1580 ± 30

usually well defined, its susceptibility shows that it corresponds to domains with M_s perpendicular to the applied field. The distortion for this series depends on φ . A second, ill-defined broader component is also observed. This corresponds to domains which are rotated in the (\mathbf{a}, \mathbf{b}) plane to directions which are intermediate between $[100]$ and the direction perpendicular to the applied field. The peak of this component, i.e., the center of the distribution is not at the position expected for a domain remaining along a $[100]$ direction. The intensity of the broad component decreases only slowly with increasing field. Contrary to the case of $\varphi=0$, for $\varphi=\pi/4$ and $\theta=\pi/2$ some fine-structure lines of the broader component were observed even at 8.1 T.

E. Temperature dependence

Little temperature dependence has been observed between 10 and 150 K. Below 10 K the Gd^{3+} spin-lattice-relaxation time becomes long and saturation effects distort the line shapes. No temperature dependence of the magnetic susceptibility is observed and the largest tetragonal crystal-field parameter b_2^0 changes by a few % between 25 and 150 K (Table I). At temperatures above 100 K a homogeneous broadening is observed which is the same for all lines. The domain structure remains well visible even at 150 K with about the same ratio for the intensities of the two series. Above 150 K the signal intensity was too small for meaningful measurements.

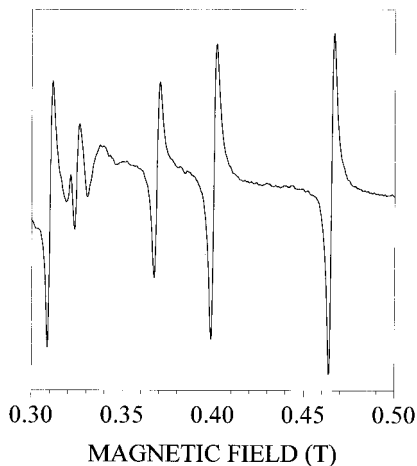


FIG. 4. Proof that the orthorhombic distortion is along $[100]$. $\text{Gd:YBa}_2\text{Cu}_3\text{O}_{6+x}$ ESR spectrum at 25 K and 9 GHz with magnetic field in the $[110]_t$ direction. In contrast to Fig. 2(a) the fine-structure lines are not split, showing that the $[110]$ and $[\bar{1}\bar{1}0]$ directions are equivalent.

F. Reproducibility and reversibility of the domain structure

The spectra of two crystals are strictly reproducible. Several runs have been made and the spectra were always independent of thermal and magnetic history. We present three experiments to demonstrate the stability of the domain structure at a given magnetic field.

The first example, Fig. 6(a), shows reversibility after a sweep to high magnetic fields. The same spectra were recorded at magnetic fields around 2.7 T in the \mathbf{a}_t direction before and after sweeping the field to 8 T. The broader fine-structure series, i.e., domains with magnetization approximately parallel to the field were entirely wiped out at 8 T. The second experiment [Fig. 6(b)] shows that rotation of the magnetic field by $\Delta\varphi=\pi/2$ in the (\mathbf{a}, \mathbf{b}) plane of the crystal does not change the 9 GHz ESR spectrum at 77 K. In the case shown in the figure the sample was rotated *in situ*. However, the same result was found at 75 GHz and 25 K where before rotation the crystal was heated to ambient temperature. The insensitivity of the spectrum to an interchange of the two principal axes is not a trivial observation. It shows that the amount of parallel and perpendicular domains is the same for the two equivalent directions of magnetic fields although rotation of the crystal in a magnetic field rearranges the domain structure and local distortions are changed by an interchange of the principal axes. In a third experiment we

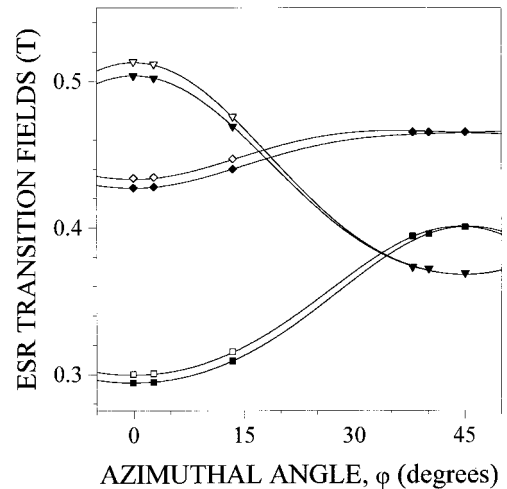


FIG. 5. Angular dependence in the (\mathbf{a}, \mathbf{b}) plane of three of the fine-structure resonance fields at 9 GHz and 77 K. $\varphi=0$ and $\varphi=45^\circ$ correspond to magnetic field in the $\mathbf{a}_t=[100]_t$ and $[110]_t$ directions, respectively. Open symbols: $H\parallel M$, full symbols: $H\perp M$. (Between 30 and 45 degrees the splitting is not resolved). Solid lines are curves calculated using crystal-field parameters of Table I.

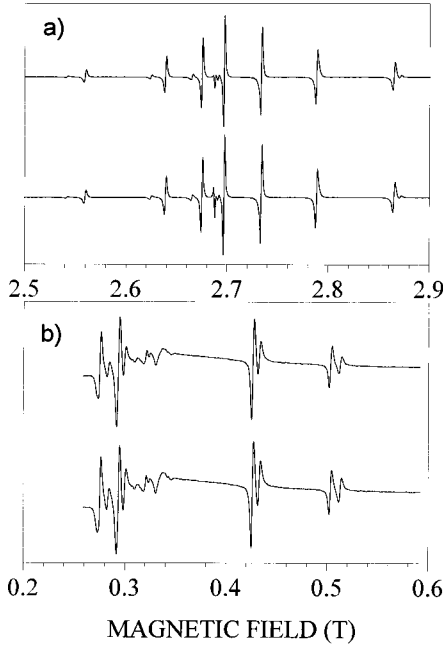


FIG. 6. Absence of magnetic hysteresis of the domain structure. (a) spectra at 75 GHz and 25 K are the same before (upper spectrum) and after (lower) $M\parallel H$ domains were wiped out at 8 T. (b) spectra at 9 GHz and 77 K are unchanged by a rotation of the magnetic field by 90 degrees in the **(a,b)** plane. The upper and lower spectra correspond to spectra with magnetic field along the two **a**_i directions fixed to the crystal. During the rotation of the field the domain structure is changed.

showed that cooling the sample through the Néel temperature in a magnetic field does not affect the domain structure. The ESR spectra of the crystal at 9 GHz and $T=125$ K were the same before and after cooling from 420 K in a magnetic field of 1 T.

V. DISCUSSION

A. Magnetic structure of $\text{YBa}_2\text{Cu}_3\text{O}_{6+x}$

Below $T_N=420$ K, the Néel temperature¹⁶ of pure $\text{YBa}_2\text{Cu}_3\text{O}_{6+x}$, Cu^{2+} ions form a simple square lattice AF order. Magnetic moments are oriented⁴ in the **(a,b)** plane but the full magnetic structure, and in particular the easy magnetization direction, has not been determined by neutron diffraction. ^{63,65}Cu(1) NQR (nuclear quadrupole resonance) shows¹⁷ that in pure $\text{YBa}_2\text{Cu}_3\text{O}_{6+x}$ with small values of x , the order along **c** is antiferromagnetic at all temperatures below T_N . Small amounts of magnetic impurities substituting nonmagnetic Cu(1) atoms [halfway between Cu(2)O₂ AF bilayers] change¹⁸ the order along **c** at low temperatures. In impure samples there is a transition^{5,18} in the interbilayer order along **c** from antiferromagnetic at higher temperatures to ferromagnetic at low T .

Our results show unambiguously that the easy magnetization direction is along [100]. Anisotropic interactions between Cu(2) magnetic moments oriented in the **(a,b)** plane distort the tetragonal symmetry of the crystal. The anisotropy is intrinsic to the layers and arises mostly from anisotropic exchange (i.e., spin-orbit interactions). In the square lattice

the magnetic dipolar interaction does not contribute to the in-plane anisotropy; in the distorted lattice, it may add to the anisotropy.

As discussed above (Sec. III), we attribute the anisotropy of the shift in the **(a,b)** plane to the anisotropy of the spin susceptibility of the AF bilayers. The low-temperature susceptibility along the easy magnetization direction of an antiferromagnet is small. If we assume that χ_a is negligible then the resonance position of Gd^{3+} without magnetic interactions (Table II) is at $^aK=1200$ ppm. This agrees well with $^{ab}K=1300$ ppm measured¹⁰ in the **(a,b)** plane of the high-temperature superconductor, Gd:YBa₂Cu₃O₇ well below T_c where the spin susceptibility is also small. From the anisotropy of the shift, $\Delta K=^bK-^aK=-2150\pm 125$ ppm, and from Eq. (3) we find $\chi_b-\chi_a=1.4\times 10^{-4}$ emu/mole for the anisotropy of the in-plane static magnetic susceptibility. The coupling constant, $^{\text{Gd}}A=-15$ (emu/mole)⁻¹ has been determined¹⁰ from a comparison of the static susceptibility and Gd^{3+} ESR shift measurements of YBa₂Cu₃O₇ in the normal state.

With the assumption of two uncoupled 2D Heisenberg antiferromagnetic Cu(2)O₂ layers in a unit cell and using the notation of Refs. 5 and 19 the static perpendicular susceptibility is

$$\chi_b = Z_\chi N_A (g_a \mu_B)^2 / (J_0 z).$$

N_A is the Avogadro number and $z=4$ is the in-plane O coordination number of Cu(2). g_a is the g factor of the Cu moments along **a**. Z_χ is the quantum renormalization factor for the susceptibility. We obtain an unrenormalized value of $J_{0u}=240$ meV with the assumptions of $g_a=2.06$ (Ref. 20) and $Z_\chi=1$. The unrenormalized value obtained from inelastic neutron diffraction is⁵ 120 meV. Renormalization improves the agreement between the two experimental values. A renormalization factor of $Z_\chi=0.448$, has been calculated¹⁹ for an isotropic two-dimensional (2D) Heisenberg antiferromagnet, the renormalized exchange energy is $J_0=108$ meV. A much smaller renormalization factor of $Z_c=1.158$ has been found¹⁹ for the spin velocity. Both renormalization factors disregard the effect of intrabilayer exchange. The anisotropy of the shift in the **(b,c)** plane is four times smaller than in the **(a,b)** plane (Fig. 7) and may arise from an anisotropy in the spin susceptibility, in the coupling constant $^{\text{Gd}}A$ or in the g factor. The obvious reason for an anisotropy of the spin susceptibility is the anisotropy of the g factor. For Cu^{2+} in various perovskite-type environments, typically $^{\text{Cu}}g_a=2.06$, $^{\text{Cu}}g_c=2.26$,²⁰ and since the spin susceptibility depends on g^2 this alone may explain the 25% difference between χ_b and χ_c .

In magnetic fields of 8 T applied along the [010] direction both M_x and the principal axis of distortion are along the unique [100] direction, i.e., perpendicular to the field in the whole crystal. The distortion may be inferred from the high-field spectra alone (i.e., without the observation of the domain structure at lower fields), since fits to the spectra with field in the [010] and [001] directions are only consistent if an orthorhombic term, b_2^2 , is taken into account. The observed orthorhombic distortion is related to magnetostriction in the CuO₂ plane and not to defects or oxygen chain fragments. We have not observed any orthorhombic distortion

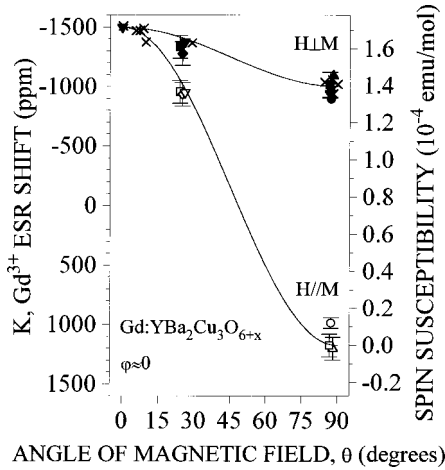


FIG. 7. Anisotropy of the Gd^{3+} ESR shift in $\text{Gd:YBa}_2\text{Cu}_3\text{O}_{6+x}$. The polar angle $\theta=0$ corresponds to $H\parallel c$. $\theta=90$ degrees corresponds to H in the \mathbf{a} , directions. $H\parallel M$ and $H\perp M$ for $\theta=90$ degrees correspond to the shift in domains where $H\parallel\mathbf{a}$ and $H\parallel\mathbf{b}$, respectively. For $\theta=90$ the shift anisotropy is proportional to the anisotropy of the spin susceptibility (see text).

fixed to the lattice (e.g., due to oxygen chains or chain fragments). Such a distortion would broaden or split the Gd^{3+} lines at high fields as much as at low fields.

Crystal-field parameters are not related in a simple way to the lattice parameters and we do not know whether the lattice is contracted or elongated along the easy magnetization direction. The ratio of the orthorhombic crystal-field parameter to the most important tetragonal parameter, $b_2^2/b_2^0=0.038$, is small. This indicates that the lattice distortion is small and it may be difficult to observe it. Indeed, no orthorhombic distortion coupled to the AF magnetization has yet been observed by diffraction methods. Magnetostriction in antiferromagnetic $\text{Gd:La}_2\text{CuO}_4$ has been suggested to be the reason for small deviations of Gd^{3+} resonance fields from crystal-field theory.²¹

B. AF domain structure

In zero or small magnetic fields the single crystal breaks up into domains with perpendicularly oriented $[100]$ easy magnetization directions. This is an observation of magnetic domains in the antiferromagnetic cuprates. The domain structure is easily modified by applied magnetic fields. As the field is increased M_s rotates and tends to be perpendicular to the field. From the ESR spectra we cannot tell the size of domains and domain walls nor whether domain walls lie parallel or perpendicular to the (\mathbf{a},\mathbf{b}) plane. We discuss below two very different scenarios: (i) mobile domain walls perpendicular to the (\mathbf{a},\mathbf{b}) plane, and (ii) fixed domain walls in the (\mathbf{a},\mathbf{b}) plane.

1. Magnetic domains separated by charged domain walls

Domain walls which separate domains within the (\mathbf{a},\mathbf{b}) plane may be formed by localized holes ordered within the CuO_2 magnetic layers. The model is motivated by the suggestion of Schultz²² for the ground state of a nearly half-filled band antiferromagnet and by the observations by Tranquada *et al.*²³ of magnetic “stripes” separated by charged

domain walls in the $\text{La}_{1.48}\text{Nd}_{0.4}\text{Sr}_{0.12}\text{CuO}_4$ perovskite. The existence of holes in the crystals due to a nonstoichiometric oxygen concentration is a natural assumption.

A single hole introduced to the valence band is a mobile singlet²⁴ which perturbs the antiferromagnetic pattern to long distances.²⁵ Schultz²² suggested that the ground state of a 2D antiferromagnet in the Hubbard model close to half band filling is insulating in spite of the finite hole concentration. In this model commensurate antiferromagnetic domains are separated by walls where the phase of the magnetic order parameter changes. Holes segregated into the domain walls have lower energy than mobile holes in the conduction band. At higher hole concentrations the ground state is an incommensurate spin-density wave.

This model explains that the domain structure is an intrinsic property of the crystal and is independent of thermal or magnetic history. The stability of the charge transfer to the CuO_2 planes assures that although domain walls formed by holes may be rearranged, they cannot be *destroyed* by a magnetic field. Temperature does not affect the charge transfer and we expect that domain walls formed by holes exist up to the Néel temperature. Indeed, we have observed no change up to 150 K in the ratio of the two types of domains. (Gd^{3+} lines are lifetime broadened above 150 K and we cannot tell the temperature up to which the domain structure exists). Below T_N a gradual inhomogeneous increase of the ^{89}Y NMR linewidth has been observed,¹¹ which we relate to the development of a small inhomogeneous distortion of the magnetic structure as domain walls become static.

The above idea assumes that magnetic domain walls (soliton walls) are easily moved by a magnetic field. Domains with M_s parallel to the field diminish and perpendicular domains increase in an increasing magnetic field. Long-range Coulomb forces between domain walls present a serious difficulty for the interpretation since domain walls of the type described by Schultz are densely charged. The charge at Cu atoms along the wall would make the structure extremely rigid. Thus, for the above picture to be valid the charge of the walls must be redistributed into a quasihomogeneous background by polarization of some other electrons.

Localization of holes and their ordering into walls is not in contradiction with other local measurements. Delocalized nonmagnetic holes would decrease the magnetic moment at all $\text{Cu}(2)$ sites as x is increased. In contrast, for most of the $\text{Cu}(2)$ atoms, no change of the magnetic moment within 0.2% has been observed²⁶ by zero field $^{63,65}\text{Cu}$ NMR for oxygen concentrations less than $x=0.2$. For higher x the number of $\text{Cu}(2)$ atoms with full moment decreases rapidly. μSR experiments²⁷ also show little change of the $\text{Cu}(2)$ moment with x in the range of $0 < x < 0.2$. This indicates that the number of atoms in domain walls becomes comparable to the number of atoms in commensurate regions at about $x=0.2$.

2. Domains separated by defective (\mathbf{a},\mathbf{b}) planes

In an alternative model, defective (\mathbf{a},\mathbf{b}) planes divide the crystal into large sections of antiferromagnetic material with no further structural defects. Nonmagnetic layers with excess oxygen ordered into $\text{Cu}(1)\text{-O}$ chains may form the dividing planes. Although we have no direct evidence for such layers, this model explains all observations with reasonable parameters.

M_s is homogeneous in the (\mathbf{a}, \mathbf{b}) plane, it lies in this plane, but it may rotate around the \mathbf{c} direction. φ_i denotes the angle of rotation from the $[100]$ direction in the i th bilayer. Except for the immediate vicinity of the defect planes, the energy of the spin system is

$$E = N_b \sum_i [-J_2 \cos(\varphi_i - \varphi_{i+1}) - (\Delta\chi H^2 / 2N_a) \times \sin^2(\varphi_i) + K_a \sin(4\varphi_i)], \quad (7)$$

where N_b is the number of Cu(2) ions per bilayer, J_2 the interbilayer exchange energy, $\Delta\chi = \chi_b - \chi_a$ is the anisotropy of the antiferromagnetic spin susceptibility, N_a is the Avogadro number, and K_a is the fourfold anisotropy energy (related to the distortion). The defect planes represent a local twofold anisotropy, they fix the direction of the orthorhombic distortion in their vicinity and thus pin the easy magnetization direction. We assume a strong pinning at the defect planes, which is taken into account as a boundary condition for the minimization of Eq. (7). The orientation of the bordering defect planes affects φ_i . Without an applied field, M_s is oriented uniformly along one or the other possible \mathbf{a} directions in some isolated sections, while in others, it has to rotate around \mathbf{c} with a $\pi/2$ or π twist to accommodate for the pinning at the two bordering defect planes. In an applied magnetic field H , Zeeman energy is gained by the rotation of M_s and twists appear in the originally homogeneously magnetized sections, and in the others the already existing twists get distorted. Anisotropy makes the twists sharper since regions with $\varphi \approx \pi/4$ are unfavorable. At small fields the fine-structure lines are split in two, corresponding to regions with M_s oriented along $\varphi \approx 0$ and $\varphi \approx \pi/2$. At high fields M_s is perpendicular to the field almost everywhere.

Figure 8 demonstrates the change of the domain structure with magnetic field for an average section length l of the order of 100 lattice constants c_0 . The figure shows simulated fine-structure line shapes for a section with a $\pi/2$ twist and with field applied along $[100]$ and $[010]$ at the two pinning layers, respectively. (Sections with a $\pi/2$ twist have the same line shapes as sections with a π or a field-induced π twist in this geometry). We calculated φ_i from a continuum approximation of Eq. (7), from which the number of spins with given φ , $dn/d\varphi$ can be derived analytically. To simulate the ESR line shape, one has to know the variation of the crystal-field parameters as a function of φ . For simplicity, we assumed that the orthorhombic distortion rotates with M_s and its magnitude is independent of φ . Spectra with high fields in the $[110]$ direction support this idea. Using this assumption, the shift of the Gd^{3+} resonance frequency is $\Delta\omega_r = Bb_2^2 \cos 2\varphi + \text{Gd} \Delta\chi \gamma H \sin^2\varphi$ where B is a numerical factor which depends on the transition chosen. We convoluted the line with a Lorentzian with a width of 2 mT to simulate the natural linewidth. In the simulation of Fig. 8 $\chi_b - \chi_a = 1.4 \times 10^{-4}$ emu/mole, $J_2 = 10^{-1}$ K, (Ref. 5) and section length, $l = 70c_0$. The anisotropy energy, $K_a = 10^{-3}$ K, is chosen so that for layers with M_s turned $\varphi = \pi/4$ from the easy direction, the Zeeman energy gain at $H = 8$ T is about balanced by the loss due to magnetostriction. With these parameters the magnetic-field dependence

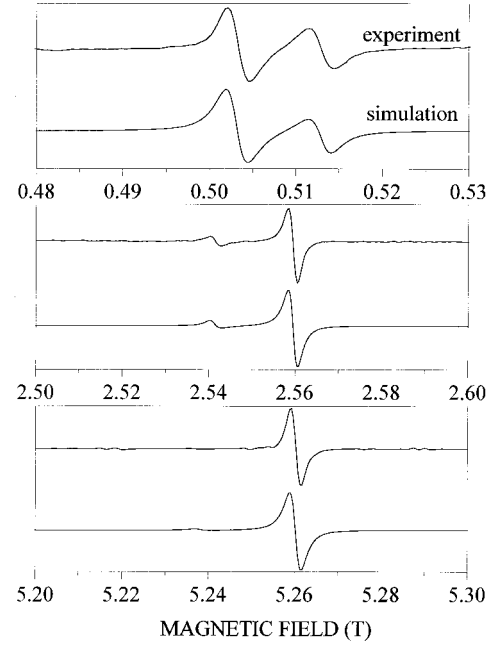


FIG. 8. Comparison of experimental line shapes with a simulation using the model of sublattice magnetization pinned to defective (\mathbf{a}, \mathbf{b}) planes separated by 70 lattice constants along \mathbf{c} . Parameters of the simulation are given in the text. The experimental spectral lines are sections of spectra shown in Figs. 2(a)–2(c).

follows well the observations for H along \mathbf{a}_r . The component of the line corresponding to $\varphi \approx 0$ decreases as field increases to $H = 0.3$ T and is nearly completely wiped out at 8 T. Although we have not performed full line-shape simulations for H along $[110]$, $dn/d\varphi$ may be calculated for this case also. In agreement with observation, the value of $K_a = 10^{-3}$ K ensures that for $H = 8$ T along $[110]$, M_s is far from being rotated perpendicular to the field in most of the section. The model does not rule out hysteresis for a magnetic-field cycle in general, but for the parameters of Fig. 8 no hysteresis occurs.

VI. CONCLUSIONS

Using Gd^{3+} spin resonance at several frequencies in high quality $\text{Gd:YBa}_2\text{Cu}_3\text{O}_{6+x}$ single crystals we determined the anisotropic spin susceptibility of the antiferromagnetic CuO_2 layers. We discussed the difference between the \mathbf{c} hard-axis and \mathbf{a} easy-axis susceptibilities in terms of a Heisenberg antiferromagnet. The need to include orthorhombic crystal-field parameters in the analysis is a clear evidence for a distortion of the tetragonal symmetry. The distortion depends on the orientation of the sublattice magnetization, M_s . Thus the distortion is a result of an intrinsic magnetostriction and is not caused by imperfections or oxygen chains in the Cu(1) layers. Magnetostriction may be important for antiferromagnetic fluctuations in the related hole-doped superconductors. An antiferromagnetic domain structure is observed. Unfortunately we cannot tell from the experiment the orientation and separation of domain walls. A model of charged domain walls—inspired by recent evidence for “stripes”

of charged and magnetic domains—fails to explain the sensitivity of the domain structure to external magnetic fields. A very different model which assumes that pure anti-ferromagnetic sections are interrupted by defective layers in the **(a,b)** plane, qualitatively explains the magnetic-field dependence.

ACKNOWLEDGMENTS

Support by the Hungarian state grants OTKA T 015984 and FKFP 0352/1997 and by the E.P.S.R.C. for the National Crystal Growth Facility for Superconducting Oxides at Oxford is gratefully acknowledged.

-
- ¹N. Nishida *et al.*, Jpn. J. Appl. Phys., Part 2 **26**, L1856 (1987); J. Phys. Soc. Jpn. **57**, 722 (1988).
- ²M. Tranquada, D. E. Cox, W. Kunman, H. Moudden, G. Shirane, M. Suenaga, P. Zolliker, D. Vaknin, S. K. Sinha, M. S. Alvarez, A. J. Jacobson, and D. C. Johnston, Phys. Rev. Lett. **60**, 156 (1988).
- ³W.-H. Li, J. W. Lynn, H. A. Mook, B. C. Sales, and Z. Fisk, Phys. Rev. B **37**, 9844 (1988).
- ⁴M. Tranquada, A. H. Moudden, A. I. Goldman, P. Zolliker, D. E. Cox, G. Shirane, S. K. Sinha, D. Vaknin, D. C. Johnston, M. S. Alvarez, A. J. Jacobson, J. T. Lewandowski, and J. M. Newsam, Phys. Rev. B **38**, 2477 (1988).
- ⁵S. Shamoto, M. Sato, J. M. Tranquada, B. J. Sternlieb, and G. Shirane, Phys. Rev. B **48**, 13 817 (1993).
- ⁶M. T. Causa, C. Fainstein, G. Nieva, R. Sanchez, L. B. Steren, M. Tovar, R. Zysler, D. C. Vier, S. Schultz, S. B. Oseroff, Z. Fisk, and J. L. Smith, Phys. Rev. B **38**, 257 (1988).
- ⁷D. Shaltiel, S. E. Barnes, H. Bill, M. Francois, H. Hagemann, J. Jegoudez, D. Lovy, P. Monod, M. Peter, A. Revcolevschi, W. Sadowski, and E. Walker, Physica C **161**, 13 (1989).
- ⁸A. Jánossy, A. Rockenbauer, and S. Pekker, Physica C **167**, 301 (1990).
- ⁹A. Rockenbauer, A. Jánossy, L. Korecz, and S. Pekker, J. Magn. Reson. **97**, 540 (1992).
- ¹⁰A. Jánossy, L.-C. Brunel, and J. R. Cooper, Phys. Rev. B **54**, 10 186 (1996).
- ¹¹H. Alloul, T. Ohno, and P. Mendels, Phys. Rev. Lett. **63**, 1700 (1989).
- ¹²S. Pekker, A. Janossy, and A. Rockenbauer, Physica C **181**, 11 (1991).
- ¹³F. Simon, A. Rockenbauer, T. Fehér, A. Jánossy, C. Chen, A. J. S. Chowdhury, and J. W. Hodby (unpublished).
- ¹⁴A. Abragam and B. Bleaney, *Electron Paramagnetic Resonance of Transition Ions* (Clarendon, London, 1970).
- ¹⁵M. T. Hutchings, in *Solid State Physics: Advances in Research and Applications*, edited by F. Seitz and D. Turnbull (Academic, New York, 1964), Vol. 16, p. 227.
- ¹⁶H. Alloul, T. Ohno, H. Casalta, J. F. Marucco, P. Mendels, J. Arabski, G. Collin, and M. Mehdod, Physica C **171**, 419 (1990).
- ¹⁷H. Yashuoka, T. Shimizu, T. Imai, S. Sasaki, Y. Ueda, and K. Kosuge, Hyperfine Interact. **49**, 167 (1989).
- ¹⁸H. Lutgemeier, Hyperfine Interact. **61**, 1051 (1990).
- ¹⁹E. Manousakis, Rev. Mod. Phys. **63**, 1 (1991).
- ²⁰S. K. Hoffmann, B. Czyzak, and J. Stankowski, Acta Phys. Pol. A **77**, 621 (1990).
- ²¹C. Rettori, D. Rao, S. B. Oseroff, G. Amoretti, Z. Fisk, S.-W. Cheong, D. Vier, S. Schultz, M. Tovar, R. D. Zysler, and J. E. Schirber, Phys. Rev. B **47**, 8156 (1993).
- ²²H. J. Schultz, Phys. Rev. Lett. **64**, 1445 (1990).
- ²³J. M. Tranquada, B. J. Sternlieb, J. D. Axe, Y. Nakamura, and S. Uchida, Nature (London) **375**, 561 (1995).
- ²⁴F. C. Zhang and T. M. Rice, Phys. Rev. B **37**, 3759 (1988).
- ²⁵B. I. Shraiman and E. D. Siggia, Phys. Rev. Lett. **62**, 1564 (1989).
- ²⁶P. Mendels, H. Alloul, J. F. Marucco, J. Arabski, and G. Collin, Physica C **171**, 429 (1990).
- ²⁷R. F. Kiefl *et al.*, Phys. Rev. Lett. **63**, 2136 (1989).